

Electromagnetically induced transparency in systems with degenerate autoionizing levels in Λ -configuration

THUAN BUI DINH¹, WIESLAW LEOŃSKI^{*}, VAN CAO LONG¹, JAN PEŘINA JR.²

¹Quantum Optics and Engineering Division, Institute of Physics, University of Zielona Góra, ul. prof. A. Szafrana 4a, 65-516 Zielona Góra, Poland

²Institute of Physics of AS CR, Joint Laboratory of Optics, 17. listopadu 50a, 772 07 Olomouc, Czech Republic

*Corresponding author: wleonski@proton.if.uz.zgora.pl

We discuss a Λ -like model of atomic levels involving two autoionizing (AI) states of the same energy. The system is irradiated by two external electromagnetic fields (strong – driving and weak – probing). For such a system containing degenerate AI levels we derive the analytical formula describing the medium susceptibility. We show that the presence of the second AI level leads to the additional electromagnetically induced transparency (EIT) window appearance. We show that the characteristics of this window can be manipulated by changes of the parameters describing the interactions of AI levels with other ones. This is a new mechanism which leads to additional transparency windows in EIT model, that differs from the mechanism where a bigger number of Zeeman sublevels is taken into account.

Keywords: electromagnetically induced transparency, electromagnetically induced transparency (EIT), lambda configuration, autoionizing states, double Fano profile.

1. Introduction

Electromagnetically induced transparency (EIT) discovered for the first time by HARRIS and co-workers [1–3] relies on the destructive quantum interference of the transition amplitudes. Such interference leads to suppression of absorption or even to complete transmission of the resonant weak probe beam. This phenomenon arises in the presence of a second (strong) laser beam coupling coherently one of the states which participate in absorption, with some other atomic state. Some reviews concerning EIT are given in literature (see for instance [4, 5] and the references quoted therein). EIT, in its classical model, can be observed for three basic atomic levels configurations. They are Λ -, V -type and cascade (ladder) ones. In these basic schemes, a single peak of enhanced transmission, or one transparency window appear. Neverthe-

less, one can find in the literature the schemes in which additional transparency windows can appear. Such models can be potentially applied for slowing down of light pulses at various frequencies [6]. The models allowing for multiple transparency windows generation were proposed and discussed, for example in [7] (for the cascade system) and in [8, 9] (*A*-model) (and the references quoted therein).

EIT phenomena can be discussed not only for the models involving discrete levels but also for those containing continuum ones. In particular, as it was shown in [10–12], it is possible to create transparency windows for systems with autoionizing (AI) states, or equivalently, with Fano structured continua. Quite recently, in [13], the model with a single AI level was discussed in this context, and the strictly deterministic control laser field was replaced by a so-called white noise signal.

AI systems involving discrete levels located above a continuum threshold (AI levels) were considered for the first time in the classical paper by FANO [14]. Fano diagonalization, based on the Coulomb mixing of AI states with the continuum, leads to a nontrivial structure of the latter [15–17] (and the references quoted therein). Such structure can be even more complicated, leading to non-trivial effects in the photoelectron spectra, if we assume that the AI system interacts with other ones, not necessarily containing AI states [18, 19]. Such models can lead to the quantum entanglement generation, as well [20]. It should be stressed out that the models involving the structured continuum (or continua) described by the Fano profiles play an essential role in various physical processes, and have also a considerable practical meaning. Since first discussions concerning Fano models in atomic physics [14], the Fano profile has been found in several functioned materials as plasmonic nanoparticles, quantum dots, photonic crystals and electromagnetic metamaterials – for exemplary considerations concerning these problems see [21, 22] (and the references quoted therein). Discussions concerning those special properties associated with its asymmetric lineshape give us potential applications in a wide range of technologies [23]. An interesting review on Fano profiles in nanostructures is given in [24].

In this paper, we present a model comprising continuum states in which the interference between two autoionization channels leads to the appearance of additional transparency EIT windows. The mechanism presented here differs from that for the systems involving only discrete levels without continua. In particular, we will show that the presence of additional AI states can lead to new quantum interference effects. As a result, the additional EIT windows appear. Moreover, changing the parameters corresponding to the transition to (from) AI states, one can manipulate the characteristics of these windows and the distances between them. However, one should keep in mind that for some particular experimental realizations of our model, some difficulties could appear during the adjustment of the parameters involved in the problem.

The model discussed here is an extension of that involving AI resonances considered by RACZYŃSKI *et al.* [12] by including the second AI level into our considerations. As it was shown in [25–28], the presence of additional AI states can lead to new quantum interference phenomena present in the system. As a result, additional zeros can appear in long-time photoelectron spectra. In this paper, for simplicity, we

will restrict ourselves to the case when two AI levels are of the same energy, *i.e.*, they are degenerate. We will show that such interference related to the presence of additional AI level can lead to the additional EIT window appearance. Moreover, changing the parameters corresponding to the transition to (from) AI states, we can manipulate the characteristics of that window. Our model is easily expendable just by adding more than one extra AI state. In such a situation, new, supplementary transparency windows will appear.

2. The model and solution

In this section, we extend the A -like model discussed by RACZYŃSKI *et al.* [12] which contains a single autoionizing level and a flat continuum coupled to other two lower discrete levels by an external laser field. In our model, instead of the one AI level, we discuss two AI levels $|a_1\rangle$, $|a_2\rangle$ with the same energy $E_1 = E_2$. Moreover, they are embedded in the same flat continuum $|E\rangle$. All of these states are coupled by a weak probe field of frequency ω_p with a discrete level $|b\rangle$ and by a relatively strong driving control field with frequency ω_c with another level $|c\rangle$. The scheme of the model is shown in Fig. 1. The configurational coupling between the AI levels $|a_1\rangle$, $|a_2\rangle$ and flat continuum $|E\rangle$ is described correspondingly by the parameters U_1 and U_2 . We call such scheme a double- A system.

In the scheme presented here, the coupling between the excited levels $|a_i\rangle$ ($i = \{1, 2\}$) and the lower discrete ones ($|b\rangle$ and $|c\rangle$) is implemented by external laser fields. In particular, the state $|b\rangle$ is coupled to the continuum $|E\rangle$ and AI levels by a weak probe field with amplitude ε_1 , whereas the state $|c\rangle$ by a control field of amplitude ε_2 . It is well-known that non-resonant interactions with other levels lead to a level shift. Therefore, the field frequencies (especially, the frequency of the strong driving field ω_2) should be properly chosen to omit such a shift.

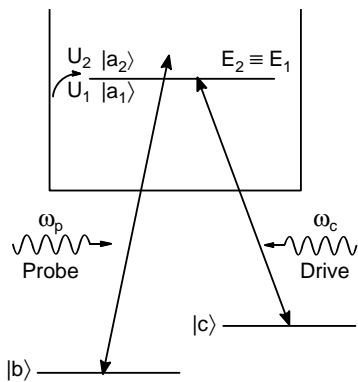


Fig. 1. Scheme of the discussed model. Due to the presence of the configurational interaction coupling (U_1 and U_2) between two AI levels $|a_1\rangle$ and $|a_2\rangle$, and the flat continuum $|E\rangle$ all these states can be replaced by the double Fano structured continuum $|E\rangle$. This continuum ($|E\rangle$) is coupled by the weak probe and strong control fields of the frequencies ω_p and ω_c , respectively.

We start from the full Hamiltonian for the system

$$\hat{H}' = \hat{H}'_0 + \hat{H}'_1 \quad (1)$$

where

$$\hat{H}'_0 = \sum_{k=1,2} \hbar \omega_{a_k} |a_k\rangle\langle a_k| + \hbar \omega_b |b\rangle\langle b| + \hbar \omega_c |c\rangle\langle c| + \int dE E |E\rangle\langle E| \quad (2a)$$

$$\begin{aligned} \hat{H}'_1 = & \left\{ \varepsilon_1 \int dE \langle E|d|b\rangle \exp(i\omega_p t) |E\rangle\langle b| + \varepsilon_2 \int dE \langle E|d|c\rangle \exp(i\omega_c t) |E\rangle\langle c| + \right. \\ & \left. + \int dE \langle E|U_1|a_1\rangle + \int dE \langle E|U_2|a_2\rangle \right\} + \text{H.c.} \quad (2b) \end{aligned}$$

where d corresponds to the electric dipole moment, whereas ε_1 and ε_2 describe strengths of the probe and control fields, respectively. Moreover, the matrix elements $\langle E|U_i|a_i\rangle$ ($i = 1, 2$) describe the configuration interaction between AI levels and flat continuum states. As usually in the papers concerning AI, we suppose now that the energies of the AI levels and the laser field frequencies are considerably higher than the energy of the threshold of the continuum. In consequence, we can neglect all threshold effects and as a result, all integrals over the energies, appearing here will be extended over the entire real axis. Moreover, we assume that all matrix elements appearing in (2) and corresponding to the transitions to (from) the flat continuum are energy independent.

It is possible to replace the subset of flat continuum states $\{|E\rangle\}$ and coupled to them AI levels $|a_i\rangle$ ($i = 1, 2$) by continuum states $|E\rangle$ (denoted here by symbols with round braces, contrary to the flat ones labeled by the usually used symbols $|E\rangle$) with some structure (density function). This function can be derived with the use of Fano diagonalization method proposed in [14] and then developed, for instance in [17]. This procedure leads to the scheme in which discrete levels $|b\rangle$ and $|c\rangle$ are coupled to the excited continuum characterized by some density of states. This density function is referred to as double Fano profile. Its shape is determined by the ratio between the matrix elements corresponding to the transitions from (to) a considered discrete level $|j\rangle$ to (from) a flat and structured continua [14, 25]:

$$\frac{\langle j|d|E\rangle}{\langle j|d|E\rangle} = \frac{(E - E_1)(E - E_2) + E(q_{1j}\gamma_1 + q_{2j}\gamma_2) - (E_1q_{2j}\gamma_2 + E_2q_{1j}\gamma_1)}{(E - E_1)(E - E_2) - iE(\gamma_1 + \gamma_2) + i(E_1\gamma_2 + E_2\gamma_1)} \quad (3)$$

where the widths $\gamma_1 = \pi|\langle a_1|U_1|E\rangle|^2$ and $\gamma_2 = \pi|\langle a_2|U_2|E\rangle|^2$ are autoionization widths of AI states. Similarly as in [25], we defined Fano asymmetry parameters q_{1j} and q_{2j} which can be expressed as:

$$q_{1j} = \frac{\langle j|d|a_1\rangle}{\pi\langle j|d|E\rangle\langle E|U|a_1\rangle} \quad (4a)$$

$$q_{2j} = \frac{\langle j|d|a_2\rangle}{\pi\langle j|d|E\rangle\langle E|U|a_2\rangle} \quad (4b)$$

where $j = b, c$. These parameters describe ratios of the direct transition between one of the lower states and AI state and its counterpart via (flat) continuum state. It follows from the form of (4) that when the direct ionization is negligible, the values of the q -parameters become high.

After performing the diagonalization procedure, the system can be described by the following Hamiltonian:

$$\hat{H}'' = \hat{H}_0'' + \hat{H}_1'' \quad (5)$$

where

$$\hat{H}_0'' = \hbar\omega_b|b\rangle\langle b| + \hbar\omega_c|c\rangle\langle c| + \int dE E|E\rangle\langle E| \quad (6a)$$

$$\hat{H}_1'' = \left\{ \varepsilon_1 \int dE (E|d|b) \exp(i\omega_p t) |E\rangle\langle b| + \varepsilon_2 \int dE (E|d|c) \exp(i\omega_c t) |E\rangle\langle c| \right\} + \text{H.c.} \quad (6b)$$

In this formula, all excited levels considered here are replaced by structured continuum states $|E\rangle$.

For further study, we derive the appropriate equations for the density matrix ρ . For this purpose, we use Liouville–von Neumann equation and apply the rotating wave approximation (RWA) [29] which allows to remove rapidly rotating terms from our set of equations. This procedure leads to the following differential equations for the matrix elements of the density matrix ρ :

$$i\hbar\dot{\rho}_{Eb} = (E - E_b - \hbar\omega_p)\rho_{Eb} - \frac{1}{2}\varepsilon_1(E|d|b) - \frac{1}{2}\varepsilon_2(E|d|c)\rho_{cb} \quad (7a)$$

$$i\hbar\dot{\rho}_{cb} = (E + \hbar\omega_c - E_b - \hbar\omega_p - i\hbar\gamma_{cb})\rho_{cb} - \frac{1}{2}\varepsilon_2^* \int \langle c|d|E\rangle \rho_{Eb} dE \quad (7b)$$

where the Fano diagonalization formalism was applied. The above equations are valid within the first order perturbation with respect to the probe field ε_1 . The parameter d appearing here is the electric atomic dipole moment and the matrix elements $\rho_{Eb} = \langle E|\rho|b\rangle$ and $\rho_{Ec} = \langle E|\rho|c\rangle$. Moreover, similarly as in [12], we have introduced the width γ_{cb} . It is a phenomenological relaxation rate for the coherence ρ_{cb} .

In general, it is possible to find the full solution of the differential Eqs. (7), but we will restrict our considerations to the long-time limit and find the steady-state solution following the way described in [12]. To solve Eqs. (7), first we eliminate ρ_{cb} expressing it in terms of ρ_{Eb} to get the integral equation which will be solved in the next step, and next, ρ_{Eb} will be found.

Since, we are interested in EIT, we should calculate the component of the electric polarization of the irradiated medium. It can be expressed as a function of the matrix element ρ_{Eb} in the following way

$$\begin{aligned}
 P^+(\omega_p) &= N \int \langle b|d|E \rangle \rho_{Eb} dE = \\
 &= -N \varepsilon_1 \left(R_{bb} + \frac{\frac{1}{4} \varepsilon_2^2 R_{bc} R_{cb}}{E_b + \hbar \omega_p - E_c - \hbar \omega_c - i \hbar \gamma_{cb} - \frac{1}{4} \varepsilon_2^2 R_{cc}} \right) = \\
 &= \varepsilon_0 \varepsilon_1 \chi(\omega_p)
 \end{aligned} \tag{8}$$

where N is the atom density, ε_0 is the vacuum electric permittivity, whereas χ is the medium susceptibility. In our model, the last can be expressed as [12]

$$\chi(\omega_p) = -\frac{N}{\varepsilon_0} \left(R_{bb} + \frac{\frac{1}{4} \varepsilon_2^2 R_{bc} R_{cb}}{E_b + \hbar \omega_p - E_c - \hbar \omega_c - i \hbar \gamma_{cb} - \frac{1}{4} \varepsilon_2^2 R_{cc}} \right) \tag{9}$$

with

$$R_{jk}(\omega_p) = \lim_{\substack{\eta \rightarrow 0^+ \\ \Delta E \rightarrow 0^+}} \int \frac{\langle j|d|E \rangle \langle E|d|k \rangle}{E_b - E + \hbar \omega_p + i \eta} dE, \quad (j, k = b, c) \tag{10}$$

The limit $\eta \rightarrow 0^+$ assures that the imaginary part of χ will be greater than zero, whereas $\Delta E = E_2 - E_1$ tends to zero for the degenerate AI levels. It is worth noting that the function inside the integral contains matrix elements corresponding to the transitions to (from) the structured continuum $|E\rangle$. Since such elements are energy dependent, we apply the formula (3) to get the explicit dependence of the integrand on the energy. Thus, we can write

$$R_{jk}(\omega_p) = \lim_{\substack{\eta \rightarrow 0^+ \\ \Delta E \rightarrow 0^+}} D_j D_k \int \frac{F_j(E) F_k(E)}{E_b - E + \hbar \omega_1 + i \eta} dE, \quad (j, k = b, c) \tag{11}$$

where the functions $F_j(E)$, $F_k(E)$ inside the integral correspond to matrix elements related to the transitions to (from) the structured continuum $|E\rangle$. The matrix elements of the dipole moment transition $\langle j|d|E \rangle$ and $\langle E|d|k \rangle$ are denoted by D_j and D_k , respectively. As it was emphasized earlier, we neglect threshold effects, so we extend the integration limits for $R_{jk}(\omega_p)$ from minus to plus infinity. Thanks to this assumption (and other mentioned earlier), we can find the analytical solution for this parameter and hence, for the medium susceptibility χ .

3. Results and discussion

Since we deal with the degenerate case, the analytical solution for $R_{jk}(\omega_p)$ can be written as:

$$R_{jk} = D_j D_k (Q_j + i)(Q_k - i) \pi \left\{ \frac{-i}{(Q_j + i)(Q_k - i)} - \frac{2i\Gamma}{(Q_j + i)(\omega + i\Gamma)} - \frac{2i\Gamma^2}{\omega^2 + \Gamma^2} + \frac{\Gamma}{\omega - i\Gamma} + \frac{\Gamma \left[Q_{j21} Q_{k21} + \Gamma_{21}^2 Q_j Q_k + \Gamma_{21} (Q_{j21} Q_k + Q_{k21} Q_j) \right]}{(1 - \Gamma_{21}^2) \left[Q_j Q_k - i(Q_j - Q_k) + 1 \right] \omega} \right\} \quad (12)$$

where the argument was redefined as $\omega = \hbar \omega_p + E_b - E_1$. Similarly as in [25], we introduced here the effective asymmetry parameters Q_j , Q_{j21} , Γ_{21} and AI width Γ defined as

$$Q_j = \frac{q_{1j}\gamma_1 + q_{2j}\gamma_2}{\Gamma}, \quad j = c, b \quad (13a)$$

$$\Gamma = \gamma_1 + \gamma_2 \quad (13b)$$

Moreover, we defined the quantities

$$Q_{j21} = \frac{q_{2j}\gamma_2 - q_{1j}\gamma_1}{\Gamma}, \quad j = c, b \quad (13c)$$

$$\Gamma_{21} = \frac{\gamma_2 - \gamma_1}{\Gamma} \quad (13d)$$

If we assume that both AI levels are characterized by the same values of parameters describing interaction between them and other levels, *i.e.*, asymmetry parameters and AI widths, the quantities $\Gamma_{21} = 0$, $Q_{b21} = Q_{c21} = 0$. In consequence, our result becomes identical to that derived by RACZYŃSKI *et al.* [12].

Further, for easier comparison of our results to those presented in [12], we take the same values for the parameters describing our system as those presented there. Thus, we assume that $\Gamma = 10^{-9}$ a.u., $D_b = 2$ a.u., $D_c = 3$ a.u. and the atomic density $N = 0.33 \times 10^{12}$ cm⁻³. Moreover, the values of the asymmetry parameters are assumed to be ~ 10 – 100 , whereas the field amplitude ε_2 is within the range from 10^{-9} to 10^{-6} a.u.

Thus, Figure 2 shows the real (dispersion) and imaginary (absorption) parts of the medium susceptibility as a function of the frequency $\omega = \omega_p + (E_b - E_1)/\hbar$ expressed in the units of Γ . Actually, we see that for the case when $\Gamma_{21} = 0$, $Q_{b21} = Q_{c21} = 0$ (solid line), we get the same result as that for the model with a single

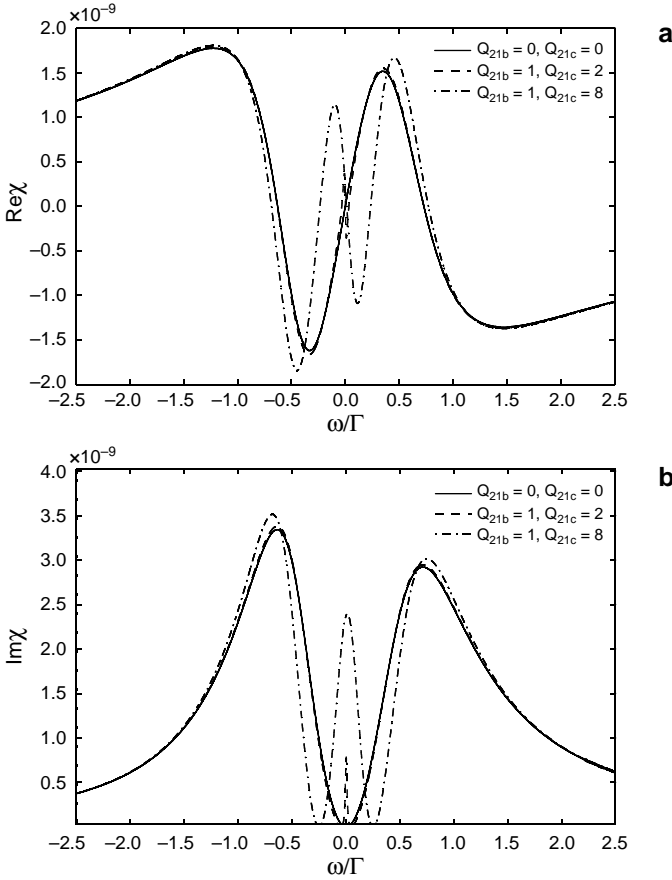


Fig. 2 The real (a) and imaginary (b) parts of the susceptibility χ as a function of the detuning ω (in units of Γ). We assume that $\varepsilon_2 = 4 \times 10^{-7}$ a.u., $\Gamma_{21} = 0$ and $Q_b = Q_c = 20$. Solid lines – $Q_{b21} = Q_{c21} = 0$, dashed lines – $Q_{b21} = 1, Q_{c21} = 2$, dashed dotted lines – $Q_{b21} = 1, Q_{c21} = 8$.

AI level discussed by RACZYŃSKI *et al.* [12]. In fact, this is the situation mentioned above, when two degenerate AI levels can be treated as a single one described by the effective asymmetry parameter and AI width. However, if we assume that the parameters describing two AI levels differ from each other, *i.e.*, $Q_{b21} \neq 0$ and $Q_{c21} \neq 0$, the situation changes considerably, because an additional zero appears in $\text{Im}\chi$, leading to the second absorption window occurrence (dashed-dotted line). In consequence, two windows are apparent and they are placed symmetrically with respect to the point $\omega = 0$. The position of these windows depends on the values of the parameters describing our system and for some cases the windows coalesce to a single one with a sharp peak inside (dashed line). Such behavior resembles that discussed in [25], concerning long-time photoelectron spectrum. The second window for our model corresponds to the additional zero in the spectrum discussed in [25] as a result of existence of extra ionization channel via the second AI level. In consequence, an addi-

tional quantum interference effect becomes present in the system leading to generation of the second zero in photoelectron spectra and the transparency window, as well. Moreover, for the system considered here one can observe an additional region of anomalous dispersion related to the presence of the second transparency window (as we compare our result with that discussed in [12]). Thus, the presence of the second AI state in the system can lead to nontrivial results, analogously to the situation presented in the discussion concerning photoelectron spectra [25–28].

The structure of created windows is very clear. It can be manipulated in potential applications, for example in simultaneous slowing down of light pulses at various frequencies [6]. In particular, the position and widths of the transparency windows can be changed by the strength of a control field. In Figure 3 we show the real and imaginary parts of the medium susceptibility again for various strengths of this field intensity ε_2 . One can see that its changes can influence the positions and widths of the windows. If we increase the value of ε_2 , both the distance between the windows

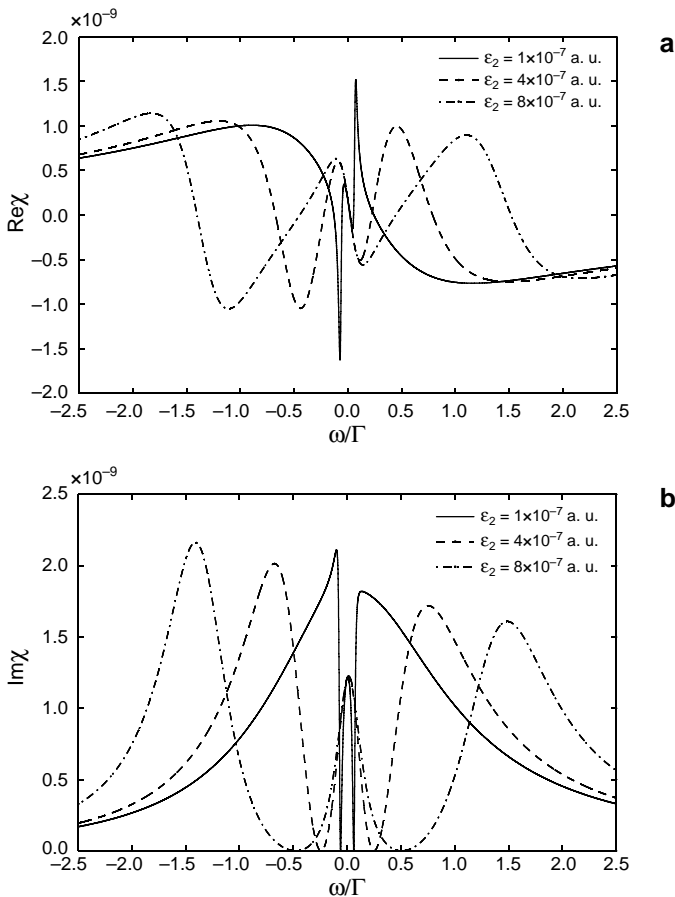


Fig. 3. The same as in Fig. 2 but for $Q_{b21} = 1$, $Q_{c21} = 8$ and various values of ε_2 . The remaining parameters are the same as in Fig. 2.

and their widths increases considerably. Thus, we can use the intensity of the control field as a control parameter for EIT effects.

In Figures 4 and 5, we show how the values of the autoionization widths can influence the number, position and width of the transparency windows. Thus, Fig. 4 corresponds to the situation when the effective asymmetry parameters $Q_{b21} = Q_{c21} = 0$. For this case, the result resembles that for the model involving single AI level, discussed in [12]. We observe only a single transparency window, and its position and width do not depend on the value of Γ_{21} . We can only observe well-defined changes in the amplitude of variations of the real and imaginary parts of χ , so the depth of the window becomes more distinct as Γ_{21} increases. However, if we assume that Q_{b21} and Q_{c21} become different from zero (see Fig. 5), the situation changes considerably again. Similarly as in Figs. 2 and 3, an additional transparency window and region of anomalous dispersion appear. From Fig. 5 we see that with increasing difference

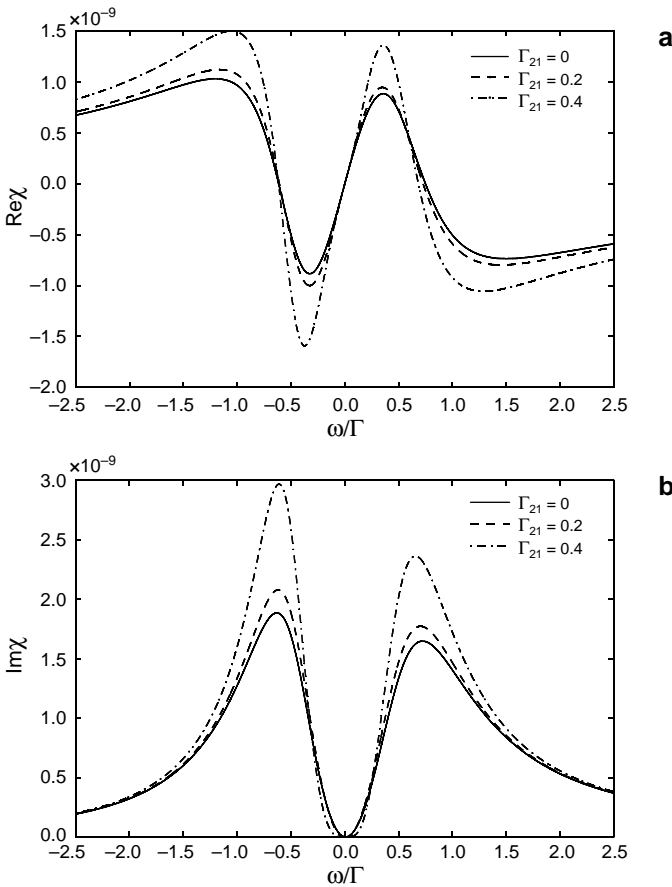


Fig. 4. The real (a) and imaginary (b) parts of the susceptibility χ as a function of the detuning ω (in units of Γ) for identical AI levels ($Q_{b21} = Q_{c21} = 0$) and various values of Γ_{21} . We assume that $\varepsilon_2 = 4 \times 10^{-7}$ a.u., and $Q_b = 15$, $Q_c = 20$.

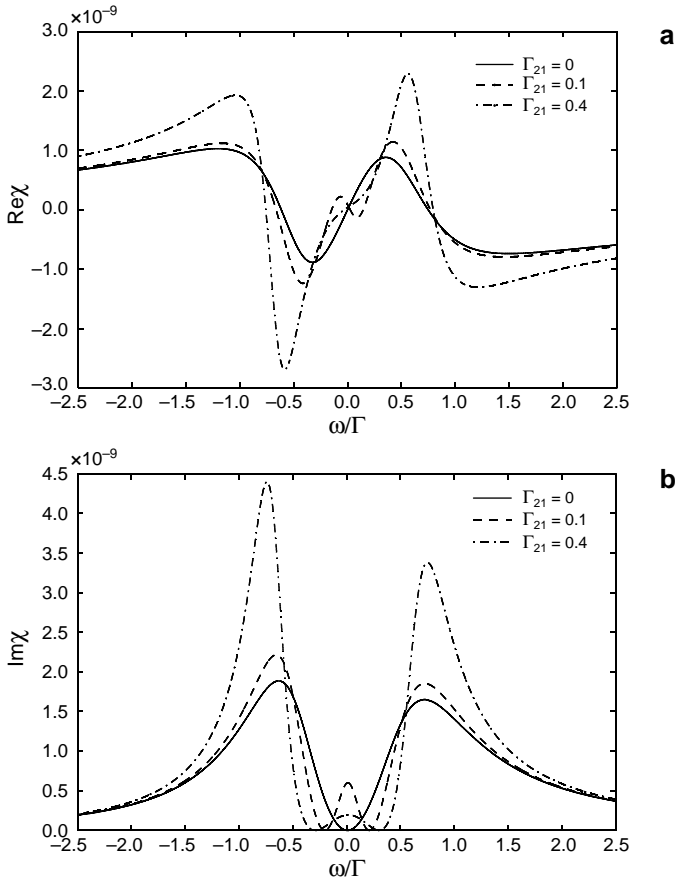


Fig. 5. The real (a) and imaginary (b) parts of the susceptibility χ for various values of Γ_{21} , Q_{b21} and Q_{c21} . Solid lines – $Q_{b21} = Q_{c21} = 0$, $\Gamma_{21} = 0$, dashed lines – $Q_{b21} = 1$, $Q_{c21} = 6$, $\Gamma_{21} = 0.1$, dashed dotted lines – $Q_{b21} = 1$, $Q_{c21} = 6$, $\Gamma_{21} = 0.4$. The remaining parameters are the same as in Fig. 4.

between the values of AI widths (Γ_{21}), the separation and widths of both windows become more pronounced. These facts justify the statements that the phenomena related to the autoionization processes strongly depend on the continuum shape and their characters. The strengths of the effects observed in the system can be changed considerably by varying the parameters describing the profile of the continuum, so we can have various possibilities of controlling these phenomena in practice.

4. Conclusions

In this paper we considered the A -like model involving two AI levels (for simplicity we assumed that they are of the same energy). This model is an extension of that with a single AI level, discussed by RACZYŃSKI *et al.* [12]. For such a model we have derived the analytical formula describing the media susceptibility χ . We have shown that due

to the presence of the second AI level we can observe an additional transparency window and extra region of the anomalous dispersion. We have shown that the properties (position and width) of the window depend on the values of the parameters describing the interaction of these levels with the driving field. Moreover, the depth of the window can be manipulated by changes of the asymmetry parameters related to the transitions induced by the probe field, they especially depend on the difference between the values of the autoionization widths. In addition, for the degenerate case, if the parameters describing two AI levels are identical, our model behaves as that with one AI level characterized by some effective AI width and asymmetry parameter. If the parameters corresponding to the two AI levels start to differ from each other, the additional EIT window appears despite the presence of degeneracy. This situation resembles that discussed in [25] concerning the long-time photoelectron spectra, when for various values of the AI level's parameters, an additional zero appeared for the degenerate case. This is a result of the existence of two channels of autoionization and quantum interference between them. Such interference disappears if two AI levels are identical. We have shown that inclusion of an additional AI state into the model can lead to new and interesting effects that are absent in the single level models.

The most important phenomenon discussed here is the appearance of the additional transparency windows in the system, where various channels of ionization (autoionization) exist. Such channels can interfere with each other giving new EIT windows. These effects could seem to be similar to those observed in the systems involving only discrete levels but they are of completely different physical character. Indeed, for the model discussed here, we deal with a structured continuum interacting with two discrete ground levels. In consequence, for the system considered here, we have a new possibility to simultaneously slowing down of light pulses at various frequencies.

References

- [1] IMAMOGLU A., HARRIS S.E., *Lasers without inversion: interference of dressed lifetime-broadened states*, Optics Letters **14**(24), 1989, pp. 1344–1346.
- [2] HARRIS S.E., FIELD J.E., IMAMOGLU A., *Nonlinear optical processes using electromagnetically induced transparency*, Physical Review Letters **64**(10), 1990, pp. 1107–1110.
- [3] BOLLER K.-J., IMAMOGLU A., HARRIS S.E., *Observation of electromagnetically induced transparency*, Physical Review Letters **66**(20), 1991, pp. 2593–2596.
- [4] FLEISCHHAUER M., IMAMOGLU A., MARANGOS J.P., *Electromagnetically induced transparency: optics in coherent media*, Reviews of Modern Physics **77**(2), 2005, pp. 633–673.
- [5] KOWALSKI K., CAO LONG V., DINH XUAN K., GŁÓDŹ M., NGUYEN HUY B., SZONERT J., *Electromagnetically induced transparency*, Computational Methods in Science and Technology, Special Issue (2), 2010, pp. 131–145.
- [6] WANG J., KONG L.B., TU X.H., JIANG K.J., LI K., XIONG H.W., YIFU ZHU, ZHAN M.S., *Electromagnetically induced transparency in multi-level cascade scheme of cold rubidium atoms*, Physics Letters A **328**(6), 2004, pp. 437–443.
- [7] KOWALSKI K., CAO LONG V., NGUYEN VIET H., GATEVA S., GŁÓDŹ M., SZONERT J., *Simultaneous coupling of three hfs components in a cascade scheme of EIT in cold ⁸⁵Rb atoms*, Journal of Non-Crystalline Solids **355**(24–27), 2009, pp. 1295–1301.

- [8] BO WANG, YANXU HAN, JINTAO XIAO, XUDONG YANG, CHANGDE XIE, HAI WANG, MIN XIAO, *Multi-dark-state resonances in cold multi-Zeeman-sublevel atoms*, Optics Letters **31**(24), 2006, pp. 3647–3649.
- [9] PAUL-KWIEK E., GLÓDŹ M., KOWALSKI K., SZONERT J., GATEVA S., VASEVA K., *Multiple peaks due to EIT and Autler-Townes effect in lambda-probing of the strongly driven $5P_{3/2}$ manifold of cold ^{85}Rb atoms in MOT*, Proceedings of SPIE **7747**, 2011, article 77470I.
- [10] VAN ENK S.J., JIAN ZHANG, LAMBROPOULOS P., *Effect of the continuum on electromagnetically induced transparency with matched pulses*, Physical Review A **50**(3), 1994, pp. 2777–2780; VAN ENK S.J., JIAN ZHANG, LAMBROPOULOS P., *Pump-induced transparency and enhanced third-harmonic generation near an autoionizing state*, Physical Review A **50**(4), 1994, p. 3362–3365.
- [11] PASPALAKIS E., KYLSTRA N.J., KNIGHT P.L., *Propagation dynamics in an autoionization medium*, Physical Review A **60**(1), 1999, pp. 642–647.
- [12] RACZYŃSKI A., RZEPECKA M., ZAREMBA J., ZIELIŃSKA-KANIASTY S., *Electromagnetically induced transparency and light slowdown for Λ -like systems with a structured continuum*, Optics Communications **266**(2), 2006, pp. 552–557.
- [13] DOAN QUOC K., CAO LONG V., LEOŃSKI W., *Electromagnetically induced transparency for Λ -like systems with a structured continuum and broad-band coupling laser*, Physica Scripta **T147**, 2012, article 014008.
- [14] FANO U., *Effects of configuration interaction on intensities and phase shifts*, Physical Review **124**(6), 1961, pp. 1866–1878.
- [15] RZAŻEWSKI K., EBERLY J.H., *Confluence of bound-free coherences in laser-induced autoionization*, Physical Review Letters **47**(6), 1981, pp. 408–412.
- [16] JOURNAL L., ROUVELLOU B., CUBAYNES D., BIZAY J.M., WUILLEUMIER F.J., RICHTER M., SLADCEK P., SELBMANN K.-H., ZIMMERMANN P., BERGERON H., *First observation of a Fano profile following one step autoionization into a double photoionization continuum*, Journal de Physique IV **3**(C6), 1993, pp. 217–226.
- [17] DURAND PH., PAIDAROVÁ I., GADÉA F.X., *Theory of Fano profiles*, Journal of Physics B: Atomic, Molecular and Optical Physics **34**(10), 2001, pp. 1953–1966.
- [18] PEŘINA J. JR., LUKŠ A., LEOŃSKI W., PEŘINOVÁ V., *Photoionization electron spectra in a system interacting with a neighboring atom*, Physical Review A **83**(5), 2011, article 053416; PEŘINA J. JR., LUKŠ A., LEOŃSKI W., PEŘINOVÁ V., *Photoelectron spectra in an autoionization system interacting with a neighboring atom*, Physical Review A **83**(5), 2011, article 053430.
- [19] PEŘINA J. JR., LUKŠ A., PEŘINOVÁ V., LEOŃSKI W., *Fano zeros in photoelectron spectra of an autoionization system interacting with a neighboring atom*, Optics Express **19**(18), 2011, pp. 17133–17142; PEŘINA J. JR., LUKŠ A., PEŘINOVÁ V., LEOŃSKI W., *Photoelectron ionization spectra in a system interacting with a neighbor atom*, Journal of Russian Laser Research **32**(5), 2011, pp. 454–466.
- [20] LUKŠ A., PEŘINA J. JR., LEOŃSKI W., PEŘINOVÁ V., *Entanglement between an autoionizing system and a neighboring atom*, Physical Review A **85**(1), 2012, article 012321.
- [21] TROCHA P., BARNAŠ J., *Quantum interference and Coulomb correlation effects in spin-polarized transport through two coupled quantum dots*, Physical Review B **76**(16), 2007, article 165432.
- [22] RIDOLFO A., DI STEFANO O., FINA N., SAIJA R., SAVASTA S., *Quantum plasmonics with quantum dot-metal nanoparticle molecules: influence of the Fano effect on photon statistics*, Physical Review Letters **105**(26), 2010, article 263601.
- [23] LUK'YANCHUK B., ZHELUDEV N.I., MAIER S.A., HALAS N.J., NORDLANDER P., GIESSEN H., CHONG TOW CHONG, *The Fano resonance in plasmonic nanostructures and metamaterials*, Nature Materials **9**(9), 2010, pp. 707–715.
- [24] MIROSHNICHENKO A.E., FLACH S., KIVSHAR Y.S., *Fano resonances in nanoscale structures*, Reviews of Modern Physics **82**(3), 2010, pp. 2257–2298.
- [25] LEOŃSKI W., TANAŠ R., KIELICH S., *Laser-induced autoionization from a double Fano system*, Journal of the Optical Society of America B **4**(1), 1987, pp. 72–77.

- [26] LEOŃSKI W., TANAŚ R., *DC-field effects on the photoelectron spectrum from a system with two autoionising levels*, Journal of Physics B: Atomic, Molecular and Optical Physics **21**(16), 1988, pp. 2835–2844.
- [27] LEOŃSKI W., BUŽEK V., *Quantum laser field effect on the photoelectron spectrum for auto-ionizing systems*, Journal of Modern Optics **37**(12), 1990, pp. 1923–1934.
- [28] LEOŃSKI W., *Squeezed-state effect on bound-continuum transitions*, Journal of the Optical Society of America B **10**(2), 1993, pp. 244–252.
- [29] ALLEN L., EBERLY J.H., *Optical resonance and Two-Level Atoms*, Wiley, 1975.

*Received November 14, 2012
in revised form January 21, 2013*